Naval Research Laboratory

Washington, DC 20375-5320

NRL/5650/MR--2021/2

A Brief Introduction to Core Modes in Optical Fiber

Frank Bucholtz

Jacobs Incorporated
Hanover, MD

Joseph M. Singley

Photonics Technology Branch
Optical Sciences Division

March 4, 2021

REPORT DOCUMENTATION PAGE

Form Approved OMB No. 0704-0188

1. REPORT DATE *(DD-MM-YYYY)* 04-03-2021	**2. REPORT TYPE** NRL Memorandum Report	**3. DATES COVERED** *(From - To)* 1 Jan 2016 – 30 Dec 2019

4. TITLE AND SUBTITLE

A Brief Introduction to Core Modes in Optical Fiber

5a. CONTRACT NUMBER

5b. GRANT NUMBER

5c. PROGRAM ELEMENT NUMBER
62271N

6. AUTHOR(S)

Frank Bucholtz and Joseph M. Singley

5d. PROJECT NUMBER

5e. TASK NUMBER
EW-271-012

5f. WORK UNIT NUMBER
6B50

7. PERFORMING ORGANIZATION NAME(S) AND ADDRESS(ES)

Naval Research Laboratory
4555 Overlook Avenue, SW
Washington, DC 20375-5320

8. PERFORMING ORGANIZATION REPORT NUMBER

NRL/5650/MR--2021/2

9. SPONSORING / MONITORING AGENCY NAME(S) AND ADDRESS(ES)

Office of Naval Research
One Liberty Center
875 North Randolph Street
Arlington, VA 22203-1995

10. SPONSOR / MONITOR'S ACRONYM(S)

ONR

11. SPONSOR / MONITOR'S REPORT NUMBER(S)

12. DISTRIBUTION / AVAILABILITY STATEMENT

DISTRIBUTION STATEMENT A: Approved for public release; distribution is unlimited.

13. SUPPLEMENTARY NOTES

14. ABSTRACT

In this report we present a brief but comprehensive introduction to the concept of core modes in optical fibers with an emphasis on the properties of the fundamental mode. We discuss such topics as the origin of modal solutions, core-guided modes in singlemode and multimode fiber, propagation effects in the presence of multiple excited core modes, and directional characteristics of splice loss. An Appendix provides further details of the fundamental mode.

15. SUBJECT TERMS

Fiber optics Optical fiber Modes Fundamental mode Step-index fiber
Singlemode fiber Multimode fiber Splice loss Photonics

16. SECURITY CLASSIFICATION OF: a. REPORT	b. ABSTRACT	c. THIS PAGE	**17. LIMITATION OF ABSTRACT**	**18. NUMBER OF PAGES**	**19a. NAME OF RESPONSIBLE PERSON**
UU	UU	UU	SAR	39	Joseph M. Singley
					19b. TELEPHONE NUMBER *(include area code)* (202) 404-1012

Standard Form 298 (Rev. 8-98)
Prescribed by ANSI Std. Z39.18

This page intentionally left blank.

Contents

(This page left blank)

1 EXECUTIVE SUMMARY

The analysis of light propagation in fibers is of great importance in telecommunications, RF signal processing, and optical sensing. This report provides a brief but comprehensive summary of the concept of core modes in fiber optic waveguides. We discuss such topics as

- the origin of modal solutions;
- core-guided modes in singlemode and multimode fiber;
- propagation effects in the presence of multiple core modes;
- directional characteristics of splice loss.

An Appendix provides further details of the fundamental mode.

It is hoped that the report will serve as an introduction for new researchers as well as a compact summary for seasoned practitioners.

This report is based on a lecture "Modes in Optical Fiber" presented by F. Bucholtz to the Optical Sciences Division in May, 2016.

(This page left blank)

2 Overview

Optical fibers are ubiquitous in today's telecommunications infrastructure and have become essential components in RF signal processing systems and optical sensing systems. The fibers are made from silica glass (amorphous SiO_2) to which dopants are added to produce a radial variation in the refractive index.

Two broad approaches are used to analyze the propagation of light in fibers: a) ray analysis, and b) electromagnetic or modal analysis, as shown schematically in Fig. 1. In our opinion, ray analyses are suitable for introductory treatments but become cumbersome and can lead to incorrect conclusions when applied to more complex problems, especially problems involving narrowband, coherent light. Modal analyses start with the differential **Maxwell's equations (MEs)**, apply the boundary conditions imposed by the fiber, and obtain all the possible solutions. Here, the solutions are called the **modes** of the fiber and, in general, there are an infinite number of modal solutions. An important subset of solutions are those that are actually guided by the fiber and, in particular, those modes that are guided by the core of the fiber. It is these modes that are most useful for physics and engineering applications and these solutions are both discrete and finite.

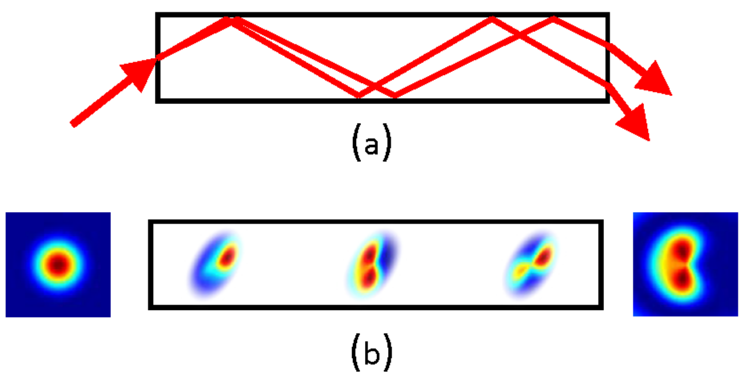

Figure 1: A schematic depiction of the two approaches for analyzing light propagation in fiber. (a) Ray analysis; (b) Electromagnetic or mode analysis.

In this report we will provide a quick, broad introduction to mode concepts in optical fiber with an emphasis on core-guided modes and, especially, on the lowest-order or fundamental mode.

Manuscript approved February 26, 2021.

3 Introduction

Suppose we are presented with the following challenge. We are handed a length of optical fiber and are given the specific form of the optical electric field $\mathbf{E}(x, y, z = 0, t)$ at the fiber input. Our task is to calculate $\mathbf{E}(x, y, z, t)$ everywhere inside the fiber as the light propagates in the z-direction (Fig. 2). The propagating field $\mathbf{E}$ is obtained by solving Maxwell's equations (MEs) subject to the appropriate boundary conditions and the general solution for a transverse, propagating wave has the form

$$E(x, y, z, t) = E_0(x, y) \cos(\beta z - \omega t) \tag{1}$$

where
$E_0(x, y)$ = field amplitude distribution in the transverse plane,
$\omega = 2\pi f$ where f is the optical frequency,
$\beta = 2\pi n_{eff}/\lambda$ = propagation constant,
n_{eff} = an effective refractive index,
λ = optical wavelength.

In writing the solution in the form of Eq.(1) we have made a number of important assumptions.

1. The light is perfectly monochromatic at optical frequency $f = \omega/2\pi$. In doing so we neglect any effects that involve spectral width such as dispersion.

2. The fiber's refractive index depends only on the transverse coordinates (x, y) and *is independent of z*. This assumption — invariance of the fiber properties on position z — is crucial in making the problem

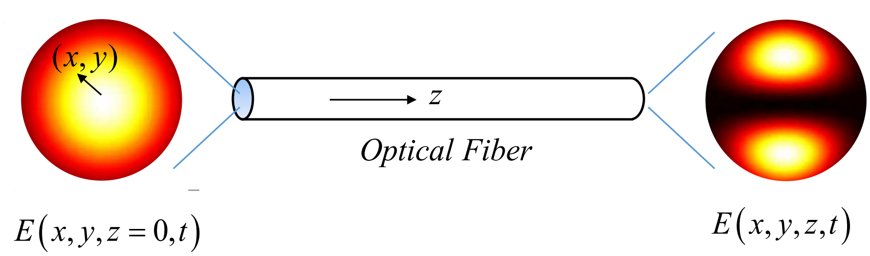

Figure 2: The challenge: Given input field $E(x, y, z = 0, t)$ to an optical fiber determine the field $E(x, y, z, t)$ at any position z along the fiber.

tractable and, as we shall see below, has far-reaching consequences for the mathematical form of the allowed solutions.

3. The electric field is a vector quantity so the solutions will be vectors $\mathbf{E} = E_x\,\hat{\mathbf{x}} + E_y\,\hat{\mathbf{y}} + E_z\,\hat{\mathbf{z}}$ and Eq. (1) shows the general form of the solution for any one of the components E_x, E_y or E_z. Later on we will see that a certain subset of the solutions called core-guided modes or just core modes can be represented to a very good approximation by just a scalar field of the type in Eq.(1). For these modes we can learn quite a bit about the mode properties by calculating just E_x or E_y — we don't need the full vector solution. Calculations with scalar fields are of course much simpler than calculations with the full vector field but, in doing so, we give up information about effects such as polarization that require knowledge of both transverse field components E_x and E_y.

4. The fiber is lossless. Otherwise a $z-$dependence would need to be included in the amplitude $E_0(x, y)$.

The transverse spatial variation of the refractive index $n(x, y)$ is *the key property* determining the optical properties of a fiber and we discuss it now in more detail. In all fibers of interest in this report, the refractive index is independent of z and has circular symmetry — its value depends only on the radial distance from the fiber center, $r = \sqrt{x^2 + y^2}$. The radial dependence of the index $n(r)$ is called the "refractive index profile" or RIP. **Once the optical frequency and RIP are specified, all the possible solutions to Maxwell's equations are locked in.**

For a standard, step-index fiber, as shown in Fig. 3, the RIP comprises a core region with index n_{co} slightly larger than the index n_{cl} of the surrounding cladding region. The core and cladding together form the glass fiber itself and, for most telecommunications fibers, have an overall diameter of 125 μm. The index values in Fig. 3 are typical for a commercial fiber called SMF-28 in which the cladding is pure silica (amorphous SiO_2) and the core is SiO_2 doped with GeO_2 to raise its index with respect to the cladding. In contrast, modern long-haul undersea cables use flourine doping in the cladding to lower its index with respect to the pure SiO_2 core. This results in a slight reduction in attenuation for the pure silica core compared to a doped-core and has significant financial benefits for multi-thousand km undersea links.

A parameter typically specified by fiber manufacturers is the so-called

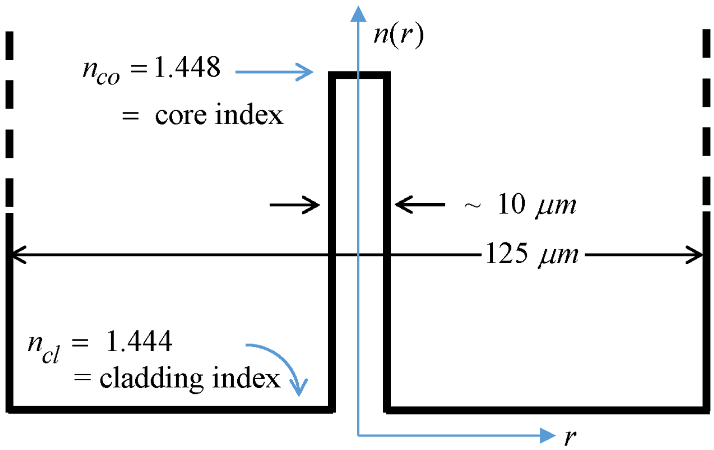

Figure 3: The refractive index profile (RIP) for a step-index fiber with index values typical for commercial SMF-28 fiber. For this fiber $\Delta = 0.0028$

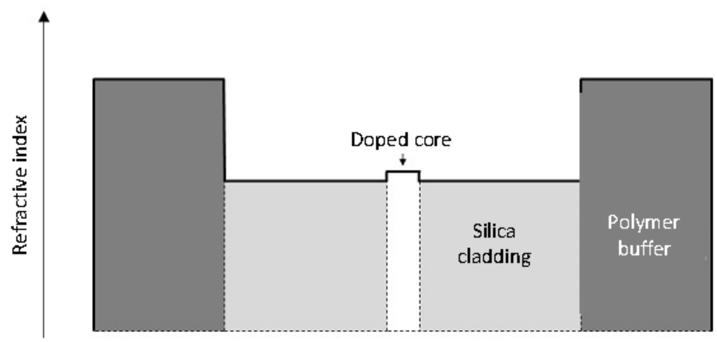

Figure 4: Showing the high-index buffer layer (jacket) applied to the outer cladding surface to both form a protective mechanical layer, to prevent ambient light from entering the fiber, and to absorb light that has escaped the core.

delta parameter,

$$\Delta = \frac{n_{co}^2 - n_{cl}^2}{2n_{co}^2}. \tag{2}$$

All of the optical fibers used for communications and for interferometric sensing are weakly-guiding fibers in which $n_{co} \approx n_{cl}$. In this case,

$$\Delta \longrightarrow \frac{n_{co} - n_{cl}}{n_{co}} << 1. \tag{3}$$

Figure 5: Some examples of RIPs. (a) Depressed cladding; (b) dispersion flattened; (c) dispersion shifted.

A typical value for a telecommunications fiber such as Corning SMF-28 is $\Delta \simeq 0.36\%$ which Corning calls the "index difference."

As a practical matter, in order to physically handle the fiber, the outer surface of the glass is coated with one or more polymer layers collectively called the jacket or buffer as shown in Fig. 4. The index of the jacket is significantly larger than that of either the core or cladding so any light that has escaped from the core and reaches the cladding-buffer interface is absorbed by the buffer instead of possibly reflecting back into the fiber. The jacket can also prevent ambient light from entering the fiber.

Depending on the intended application of a fiber, the RIP can be custom-designed to trade off various engineering parameters such as attenuation, bend resistance, and dispersion properties. A few of the myriad custom RIP designs are shown in Fig. 5. For the remainder of this report we will consider only step-index profiles.

4 Modal Solutions to Maxwell's Equations

4.1 Overview

In this section we discuss solutions to Maxwell's equations subject to the boundary conditions imposed by the RIP assuming the fiber is lossless and that its material properties don't depend on position along the fiber. Common scientific sense tells us that these last two assumptions cannot be strictly met in the real world but fabrication techniques for optical fiber have become so good that, under normal use, these assumptions are quite reasonable. Finally, as stated earlier, in this report we consider only scalar field solutions for step-index RIPs.

As with many boundary-value problems, it turns out that only certain forms of the general solution in Eq.(1) are allowed. These specific solutions are called modes. Mathematically, the **modes are eigenfunctions** (or eigenmodes or eigensolutions) of the system defined by MEs and the RIP. We will see below that, once we have the modal solutions, we can easily answer the challenge posed in the Introduction, namely, given an input field determine the field at any position along the fiber. We assumed the RIP was independent of z with the result that the amplitude of the modal field distributions $|E(x, y, z)|$ are independent of z. However, the overall phase of each mode depends strongly, but simply, on z. It is these two properties together that make the mode approach so powerful.

4.2 Modes in Step-Index Fiber

There exist three broad categories of allowed modes in optical fiber:

1. **Core modes** are modes guided by the core-cladding interface. They are discrete and finite in number.

2. **Cladding modes** are modes guided by the combination of core-cladding and cladding-buffer interfaces. They are also discrete and finite in number.

3. **Radiation modes** are unguided waves that are not confined by the fiber but are nevertheless valid solutions. These modes form a continuum and are infinite in number.

Taken together these solutions comprise the complete set of allowable solutions to our problem. Each mode is identified by a label of some sort and it will be convenient to use a pair of labels l and m. Since the guided waves are discrete their labels are integers while, for the radiation modes, the labels must be treated as continuous parameters.

Leaky modes are another type of mode are often mentioned in the literature. They are actually radiation modes that behave like cladding modes over short distance and they are useful for understanding the operation of certain devices and will be discussed in more detail below.

For the purposes of our discussion it is helpful to rewrite the scalar solution of Eq.(1) in complex form and to include the mode labels

$$E_{lm}(x, y, z, t) = e^{j(\beta_{lm} z - \omega t)} E_{0lm}(x, y). \tag{4}$$

We now summarize some important general properties of modes.

- Each mode is characterized by a specific transverse field distribution $E_{0lm}(x, y)$ and a propagation constant β_{lm} or, equivalently, an effective mode refractive index $n_{eff,\,lm} = \beta_{lm}/(2\pi/\lambda)$.

- As light propagates in any particular mode, the only change is an overall accumulation of the phase across the entire phase front at a rate per unit meter given by the propagation constant β_{lm}. The magnitude of transverse field distribution $E_{0lm}(x, y)$ remains the same everywhere along z.

- The field distribution $E_{0lm}(x, y)$ is independent of the direction of propagation which is itself determined by the sign in the argument of the exponential in Eq.(4). For waves propagating in the $+z-$direction the argument is $(\beta_{lm}z - \omega t)$ while for waves propagating in the $-z-$direction the argument is $(\beta_{lm}z + \omega t)$. In both cases the propagation constant β_{lm} is assumed to be positive.

- As mathematical functions, the modes are orthogonal and form a basis. This means that any arbitrary field distribution can be expressed as a linear combination of the modal solutions. If $E_{in}(x, y)$ is the transverse distribution of an arbitrary light beam incident on the fiber endface, then that light beam can always be written as a linear combination of the basis modes

$$E_{in}(x, y, 0) = \sum_{l,m} c_{lm} E_{0lm}(x, y) + \int_0^\infty \int_0^\infty c_{\mu\nu} E_{0\mu\nu}(x, y) d\mu d\nu \quad (5)$$

  where the c_{lm} are complex weighting coefficients and where the discrete indices l, m label the guided modes and the continuous indices μ, ν label the radiation modes. In any realistic situation many of the c_{lm} will be zero or close to zero so, typically, not all the modes are needed to represent an incident field to a high degree of fidelity. But this also means that if an arbitrary, oddly-distributed beam of light is injected into a fiber it's likely that more than one mode and possibly a great many modes will be excited. To say a particular mode (l, m) is "excited" by an input field in this context means that the coefficient $c_{lm} \neq 0$.

- Orthogonality of modes means that there is never intermodal crosstalk. Light in one mode stays in that mode. But this is in the ideal case. If there are any perturbations to the fiber such as bends, deformations, or localized composition or density fluctuations, then our carefully crafted assumption of the invariance of the index along z is invalid and crosstalk can occur. But again, today's fibers are so well designed and fabricated that this assumption is quite accurate under most circumstances.

- It sometimes happens that two modes have exactly the same propagation constant even though they have different lm labels. In this case, the modes are said to be **degenerate** and they can exchange power even in the absence of perturbations.

The complex coefficients c_{lm} in Eq.(5) are a normalized measure of how well any particular fiber mode $E_{0lm}(x, y)$ matches the incoming field distribution $E_{in}(x, y, z = 0)$. Quantitatively

$$|c_{lm}|^2 = \frac{\left|\int\int E_{in}(x, y, z = 0)E_{0lm}(x, y)dxdy\right|^2}{\int\int |E_{in}(x, y, z = 0)|^2 dxdy \int\int |E_{0lm}(x, y)|^2 dxdy}. \tag{6}$$

where the integrals are performed over the entire transverse plane. The magnitude of the c_{lm}'s are proportional to what in traditional optics is called the **overlap integral**,

$$c_{lm} \propto \int\int E_{in}(x, y, 0)E_{0lm}(x, y)dxdy. \tag{7}$$

The quantum optics folks would call this the projection of the input field onto the mode and the math folks would call this the inner product of the input field and the mode field.

Taken together, these general properties provide the great power and utility of the mode approach for propagating fields:

1. The modes form a basis so any arbitrary incident field can be expressed as a linear combination of modes.

2. Each mode then propagates along the z-direction undisturbed in amplitude, independent of all the other modes, and with a simple $z-$dependent phase term, $\exp(j\beta z)$.

3. To obtain the total field distribution anywhere along z simply propagate each mode individually up to z and then add up all the modes.

That's it! We now have almost all the tools needed to solve the challenge. What remains is to determine the actual shape of the modal solutions for a step-index fiber.

5 Core Modes in Step-Index Fiber

5.1 Basics

For core modes in general, all three vector components of the field (E_x, E_y, E_z) are non-zero and the exact solutions are messy and cumbersome. In 1971, using the weakly-guided assumption of Eq.(3), Gloge [1]

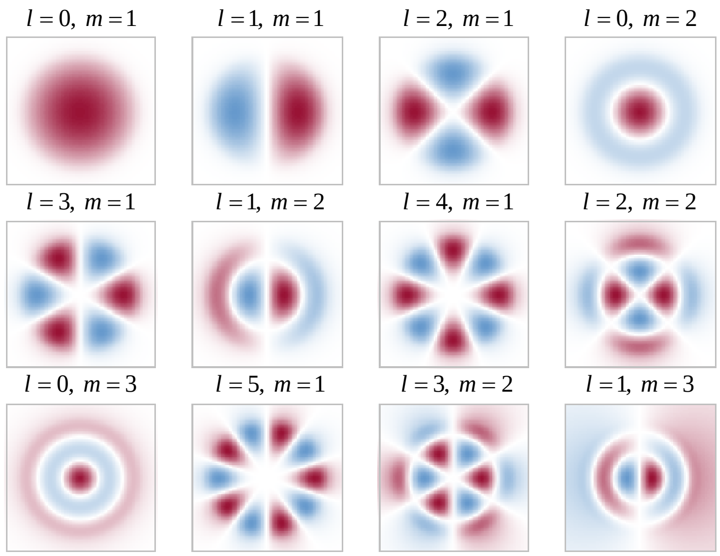

Figure 6: The transverse field distributions $LP_{lm}(x, y)$ for a few of the lower-order core-guided LP modes. Red vs blue colors indicates a relative difference in sign (π phase shift) between the fields at the two locations.

constructed a set of approximate solutions that were intended to be "good enough" for engineering applications and in which the level of accuracy was on the order of the core/cladding index difference. For these approximate solutions the transverse field ends up almost entirely in either E_x or E_y. That is, the solutions are nearly linearly polarized and these modes are thus referred to as "LP" modes. For our purposes, we will need to consider only one of the field components and thus we will deal entirely with scalar modes.

Figure 6 shows the field distribution for a few of the lower-order LP modes. We will designate the core-guided LP modes by LP_{lm}. Although the boundary condition imposed by the RIP has perfect circular symmetry we see that, in general, all the modes do not enjoy that same symmetry. Only the $l = 0$ modes are circularly symmetric. However, the remaining modes do possess rotational symmetry, where the field distribution is symmetric under rotations of $2\pi/l$ and the power distribution is symmetric under rotations of π/l.

Details of the calculation of modes in circular dielectric waveguides can be found in many excellent texts and articles. We have already cited the article by Gloge which is very readable. In addition, we recommend the

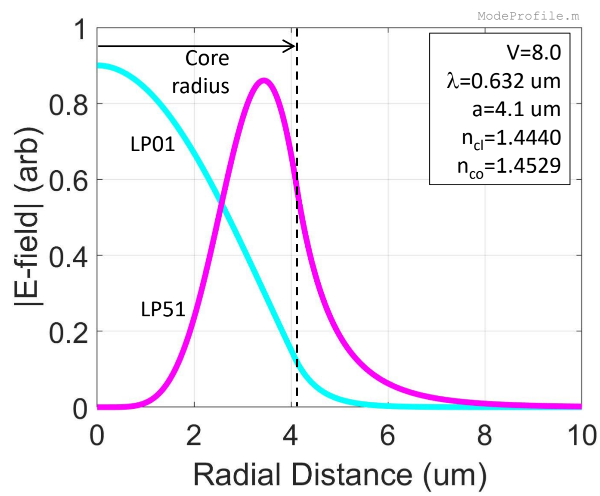

Figure 7: The mode profiles for two modes, LP01 and LP51, far from cut-off at $V = 8.0$, showing the extent to which the tail of radial field distributions can extend into the cladding. Parameters used to calculate the curves are shown in the inset.

books by Jeunhomme [2], Miller and Chenowyth [3], Unger [4], Marcuse [5], Agrawal [6], and Snyder and Love [7]. In particular, if it is required to perform computer simulations of LP modes, we recommend the Chapter by Marcuse, Gloge, and Marcatili in Miller and Chenowyth [3] and Chapter 1 in Jeunhomme [2] as good references, as well as the summary provided in the Appendix to this report.

It is important to keep in mind that the modes shown in Fig. 6 are indeed all guided by the core but they are definitely not confined entirely within the core. In fact, the tails of the field distribution of *every* core-guided mode extends into the cladding, with higher-order modes having more light near and beyond the core-cladding interface than lower-order modes. This behavior is seen in Fig. 7 which shows the radial field profile for an LP_{01} and an LP_{51} mode as examples.

We now examine some aspects of the behavior of the guided LP core modes in step-index fiber.

As mentioned earlier, the E-field distribution for any particular mode $LP_{lm}(x, y)$ remains unchanged as it propagates in the fiber. The phase of the mode does change but it changes very simply,

$$LP_{lm}(x, y, z) = e^{j\beta_{lm}z} LP_{0lm}(x, y). \tag{8}$$

That is, the phase accumulates at a constant rate β_{lm} per meter.

The mode with the largest propagation constant (largest refractive index) is by definition called the **fundamental mode**. Of all the core modes, this mode accumulates phase at the largest rate per unit length and has the lowest **phase velocity**

$$v_{phase} = \frac{\omega}{\beta} = \frac{c}{n_{eff}} \tag{9}$$

where $n_{eff} = \beta/k$ is the effective index of the mode and $k = 2\pi/\lambda$ is the wavenumber in vacuum.

On the other hand, the speed at which *power* flows in a mode is given by the mode **group velocity**

$$v_{group} = \left(\frac{d\beta}{d\omega}\right)^{-1} = \frac{c}{n_{group}} = \frac{c}{\left(n_{eff} + \omega\left(dn_{eff}/d\omega\right)\right)}. \tag{10}$$

Among all the allowable core guided modes, the fundamental mode has the smallest phase velocity, but it may or may not have the smallest group velocity. Typically it does not.

5.2 Single- vs Multi-Mode Fiber

For the remainder of this section we will consider only core-guided modes. Earlier we stated that once the optical frequency and the RIP of the fiber were specified then all the allowed modal solutions were locked in. When solving MEs for the core-guided modes in step-index fiber, an extremely useful parameter falls out naturally. It is referred to as the "**V-parameter**" or the "**normalized frequency**" and is given by

$$V = \frac{2\pi}{\lambda} a \left(n_{co}^2 - n_{cl}^2\right)^{1/2} = \omega \frac{a}{c} \left(n_{co}^2 - n_{cl}^2\right)^{1/2} \tag{11}$$

where a is the core radius and the remaining parameters were defined earlier. For a given optical frequency and RIP, the value of V determines the number of core-guided modes the fiber can support:

- If $V \leq 2.405$, there is only one core-guided solution and the fiber is called **singlemode**.
- If $V > 2.405$ more than one core-guided mode is allowed and the fiber is called **few-mode** or **multimode** depending on how many modes are allowed. But the term "multimode" is often applied to any fiber that supports more than one core mode, regardless of number.

Note that V is dimensionless and depends on the difference between core and cladding indices and on the ratio of the core radius to the optical wavelength. Also, keep in mind that the terms "singlemode" and "multimode" apply only to the core-guided modes. **A singlemode fiber can still have many allowed cladding and radiation modes**.

Each core mode is characterized by an **effective index of refraction** $n_{eff} = \beta/k$ that lies somewhere in value between the cladding and core indices,

$$n_{cl} \leq n_{eff} \leq n_{co} \tag{12}$$

as shown in Fig. 8. The exact value of the effective index between its two limits is determined by a parameter b called the **normalized propagation constant** where

$$n_{eff}^2 = (1-b)n_{cl}^2 + bn_{co}^2 \tag{13}$$

or, in the weakly-guided approximation,

$$n_{eff} \approx (1-b)n_{cl} + bn_{co}. \tag{14}$$

Hence

$$b = \frac{(\beta/k)^2 - n_{cl}^2}{n_{co}^2 - n_{cl}^2} \approx \frac{(\beta/k) - n_{cl}}{n_{co} - n_{cl}} = \frac{(n_{eff} - n_{cl})}{n_{co} - n_{cl}}. \tag{15}$$

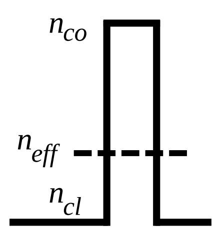

Figure 8: For a core-guided mode the effective index always lies between the cladding and core indices.

To get an overall understanding of the behavior of the LP modes it is useful to plot the propagation constant as a function of V-number. But rather than make such a plot for each particular situation, that is, for each particular combination of n_{co}, n_{cl}, λ and a, we can instead create a set of universal curves by plotting b as a function of V, as shown in Fig. 9 for a few of the lowest-order LP modes.

This plot is extremely useful and reveals at a glance a number of important properties of core-guided modes in step-index optical fibers in the weakly-guided approximation:

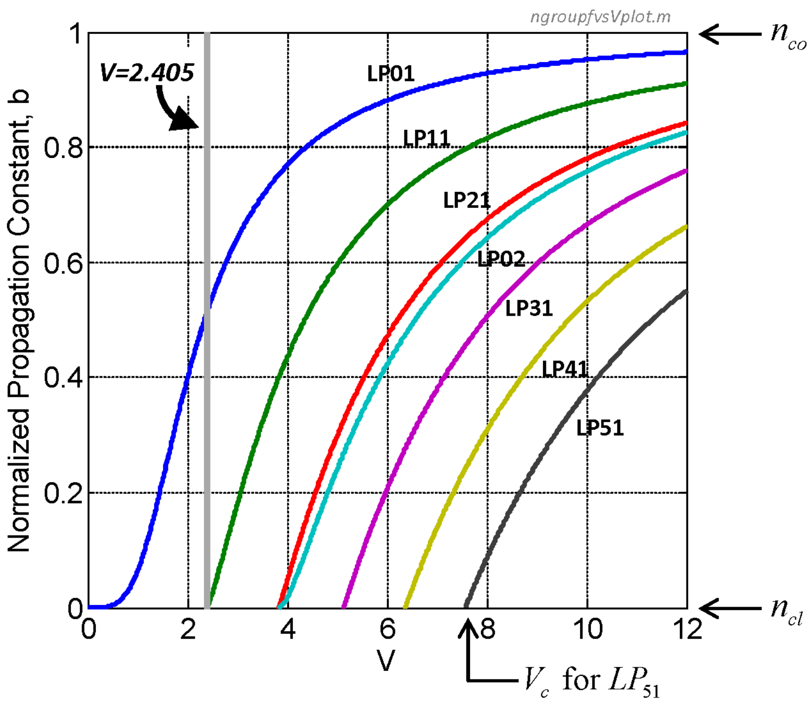

Figure 9: Normalized propagation constant b as a function of normalized frequency V for a few LP modes. n_{co} = core index, n_{cl} = cladding index, $V_c \simeq 7.6$ indicates the cut-off frequency for the LP_{51} mode as an example. The value 2.405 is especially important since the fiber supports only a single core mode when $V < 2.405$. For SMF-28 fiber at 1550 nm, for example, $V \simeq 2.0$.

- For all modes, $0 \leq b \leq 1$ which is equivalent to $n_{cl} \leq n_{eff} \leq n_{co}$ emphasizing that, for a mode to remain core-guided, its effective index must lie between the core and cladding indices.

- As V decreases, there comes a point for (almost) every mode where $n_{eff} = n_{cl}$. The wave then can't distinguish its own effective index from the cladding index and can no longer be core-guided. At this point the mode is said to **"reach cut-off"** or to **"be at cut-off"** and that mode is no longer a solution to MEs. For example, the LP_{51} reaches cut-off at approximately $V \simeq 7.6$ as seen in Fig. 9.

- For the fundamental mode, b approaches zero only asymptotically as V approaches zero.

- For $V \leq 2.405$ only the fundamental exists, all the other core modes have reached cut-off, and the waveguide is singlemode. Note that if, say, the wavelength were then decreased to the point that $V > 2.404$, then at that new wavelength the same fiber would be multimode.
- As $V \longrightarrow \infty$, the effective index of all modes approaches the core index, the waveguide is highly multimode, all the modes are far from cut-off and are strongly guided. This situation rarely occurs in practice for glass fibers since very large V-number requires either very short wavelength or very large Δ.

Hopefully the reader can see that **once you know V you know a lot!**

Before moving on we need to clarify two points in regard to Fig. 9. First, we have restricted our discussion to scalar fields and have therefore ignored polarization effects. However, for each mode there are actually two solutions in orthogonal polarization states. For an ideal fiber with perfect circular symmetry these two modes are degenerate — they have exactly the same propagation constant. However, if the symmetry is broken (due to bending or manufacturing inaccuracies, for example) then the degeneracy is removed and the two modes propagate with different constants. In the extreme case of polarization-maintaining fiber, the RIP of the fiber is purposely designed to be non-circularly symmetric so that the two modes have significantly different propagation constants. Second, to simplify the figure we plotted only some of the allowable modes in the range of V-numbers shown. LP_{22} was not plotted for example. It can be shown that for a given V-number, the number of allowable core-guided modes is approximately $N = V^2/2$, counting the two polarization modes for each scalar mode.

As an example of a plot for a specific fiber, in Fig. 10 we show the mode effective index n_{eff} vs V for a fiber having RIP similar to SMF-28 fiber where we assumed $n_{cl} = 1.444$ and $n_{co} = 1.448$

The mode group index n_{group}, which determines how fast power propagates through the fiber, depends on both the effective index and the derivative dn_{eff}/dV,

$$n_{group} = n_{eff} + V\frac{dn_{eff}}{dV}. \tag{16}$$

Figure 11 is a plot of n_{group} vs V for the same SMF-28-type fiber that was plotted in Fig. 10. We see here that the group index of the fundamental LP_{01} mode is smaller than the group index of the other modes shown over just about the whole range of V values. Hence, in the fundamental mode compared to the other modes, power propagates *fastest* per unit time while phase accumulates at the slowest rate per unit length.

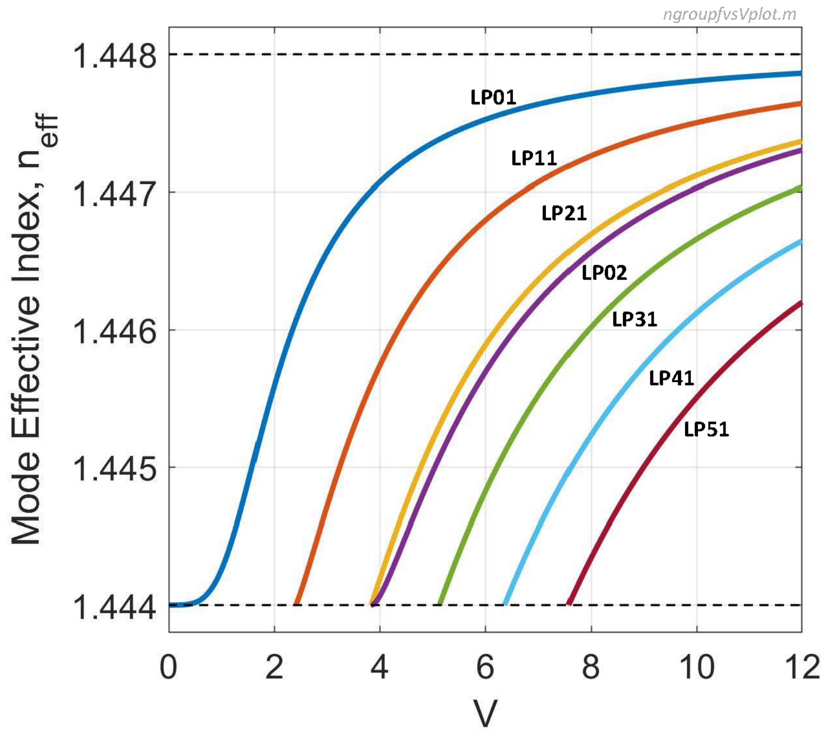

Figure 10: Mode effective index n_{eff} as a function of V for a fiber having RIP similar to SMF-28 fiber. The effective index for all modes lies between the cladding index $n_{cl} = 1.444$ and the core index $n_{co} = 1.448$ of the fiber.

Recall that one of the general properties of a mode in a lossless fiber is that the transverse field distribution $LP_{lm}(x, y)$ remains unchanged as light in the mode propagates along the fiber: there is no attenuation of the mode nor spatial redistribution of the E-field in the transverse plane. Also, referring to Fig. 9, we noted that as the value of V decreases the mode eventually reaches cut-off when $n_{eff} = n_{cl}$. Light that was propagating in a core mode that went through cut-off due, for example, to a localized mechanical deformation, typically converts into a radiation mode. But it can be a radiation mode with characteristics very close to certain cladding modes. Instead of quickly radiating away the light can propagate for quite long distances — tens of microns or more — before eventually "leaking" away. **Leaky modes** are typically not an issue in communication and RF links but they can produce unwanted interference effects in the presence of strong bends and other mechanical perturbations. Here, the mechanical

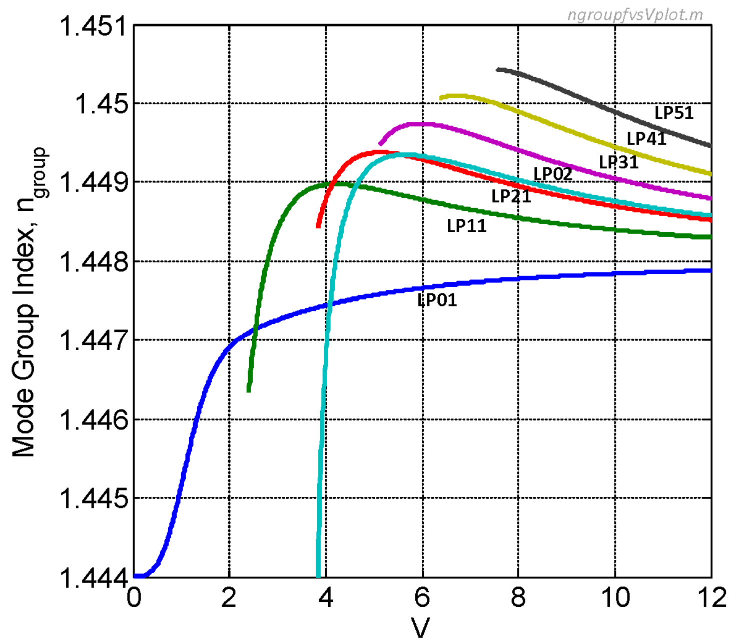

Figure 11: Mode group index n_{group} as a function of V for a few LP modes for a fiber having RIP similar to SMF-28. The fundamental mode LP_{01} has neither the largest nor the smallest group index over the range of V values shown.

disturbance puts light into a leaky-mode and it is then possible for the same disturbance to couple some light back into the fundamental mode and produce optical interference.

Finally, as if the V-number had not yet proved its worth, it is directly related to a geometrical-optics property of the fiber, namely, the acceptance angle as shown in Fig. 12. The sine of the acceptance angle θ_c is the **numerical aperture (NA)** and is given by

$$NA = \sin\theta_c = \frac{1}{2 \cdot f/\#} = \sqrt{n_{co}^2 - n_{cl}^2} = \frac{\lambda}{2\pi a}V \tag{17}$$

for air (index $n_i \approx 1$) as the input medium. (Otherwise the right-hand side of (17) must be divided by the index of the input medium n_i.) Here, $f/\#$ is the traditional $f-$number or speed of the entrance aperture of the optical fiber. Only light having $k-$vectors within the acceptance angle will propagate in the fiber as a guided mode. Note that in the case of multimode operation, $V > 2.405$, (17) gives the acceptance angle for all available modes but does not dictate how much power is injected into each mode.

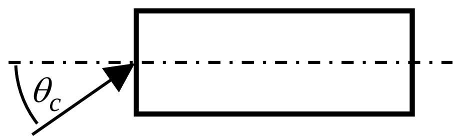

Figure 12: The critical angle θ_c defines an acceptance cone of $k-$vectors for incident light to enter the fiber and excite a guided mode.

5.3 Applications

5.3.1 Superposition of Modes

In this section we consider what happens when light in multiple core-guided modes propagate simultaneously. In particular, we calculate and compare the $z-$dependence of the total field and the total optical power. Assume that the input field comprises a sum of LP modes given by

$$E(x, y, 0, t) = \exp(-j\omega t) \sum_{l=0}^{L} \sum_{m=1}^{M} c_{lm} LP_{lm}(x, y) \tag{18}$$

where L and M are integers and the c_{lm} are complex weighting coefficients from Eq. (7). Then the field at any position z in the fiber is obtained simply by first advancing the phase of each mode individually according to its propagation constant β_{lm}, that is, $LP_{lm}(x, y) \longrightarrow LP_{lm}(x, y) \exp(j\beta_{lm} z)$, and then re-assembling all the mode fields into a total field

$$E(x, y, z, t) = \exp(-j\omega t) \sum_{l=0}^{L} \sum_{m=1}^{M} c_{lm} LP_{lm}(x, y) \exp(j\beta_{lm} z). \tag{19}$$

This result is the answer to the challenge posed at the beginning of the report. It gives the prescription for determining the field at any point along the fiber, $E(x, y, z, t)$ given a monochromatic input field $E(x, y, 0, t)$.

The distribution of optical power $p(x, y, z)$ in the transverse plane (x, y) at location z, is

$$p(x, y, z) \propto |E(x, y, z, t)|^2. \tag{20}$$

The total field at any location (x, y, z) is the sum of a number of modes, all at the same optical frequency ω but each with phase $\beta_{lm} z$. Hence, optical interference occurs at each point (x, y, z) and strong spatial variations can occur in both the transverse distribution of power for fixed $z = z_0$, and in the longitudinal distribution of power for fixed (x_0, y_0). If we took successive slices of the fiber and examined the pattern of optical power at the output we would find that it "sloshes around" quite a lot in the transverse plane as z changes on optical length scales. But if the fiber is lossless the total power - obtained by integrating $p(x, y, z_0)$ over the (x, y) plane - will be constant, independent of z.

As an example, suppose the incident field is represented by the following linear combination of LP_{01}, LP_{11}, and LP_{21} modes

$$E(x,y) = \sum_{l=0}^{\infty} \sum_{m=1}^{\infty} c_{lm} LP_{lm}(x,y) \tag{21}$$

$$= (-0.707) LP_{01}(x,y) \tag{22}$$

$$+ (0.548) LP_{11}(x,y) \tag{23}$$

$$+ (-0.447) LP_{21}(x,y). \tag{24}$$

Then the distribution of optical power just inside the fiber is

$$p(x, y, z = 0) \propto |E(x,y)|^2 \tag{25}$$

Figure 13 shows the individual mode fields, individual mode powers, total field, and total power for this example.

We can determine how both the optical field distribution and the optical power distribution evolve with z as the light propagates in the fiber. The propagation constants for each mode were obtained using the mode effective index from Fig. 10 for SMF-28 fiber. The result is shown in Fig. 14.

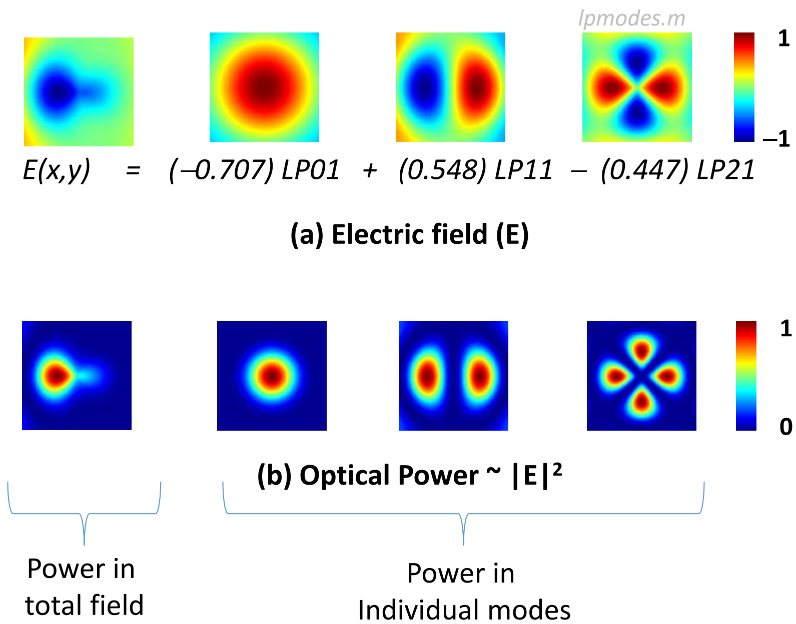

Figure 13: Showing the field and power distribution in the transverse plane for the example incident field in the text.

5.3.2 Modes and Splice Loss

Overview In this section we apply the mode concept to discuss light propagating across the interface between two fibers, a situation that occurs when two fibers are spliced together. Here we are interested in both how loss occurs and in the dependence of loss on the direction of light through the splice. The discussion will be largely qualitative.

We will see that, provided all the modes in both fibers are taken into account, all the optical power incident on the splice is present beyond the splice. Mathematically, every splice is lossless. But to the experimentalist loss means something very different. In the context of a splice joint, the term "loss" usually refers to the ratio of optical powers in the fundamental modes of two singlemode fibers on either side of the splice. More generally, it may refer to the ratio of optical power in the core-guided modes of two multimode fibers or even between a singlemode and multimode fiber. In this last case, some light from the input fiber can end up in modes in the output fiber that are not easily accessible for measurement and, hence, to

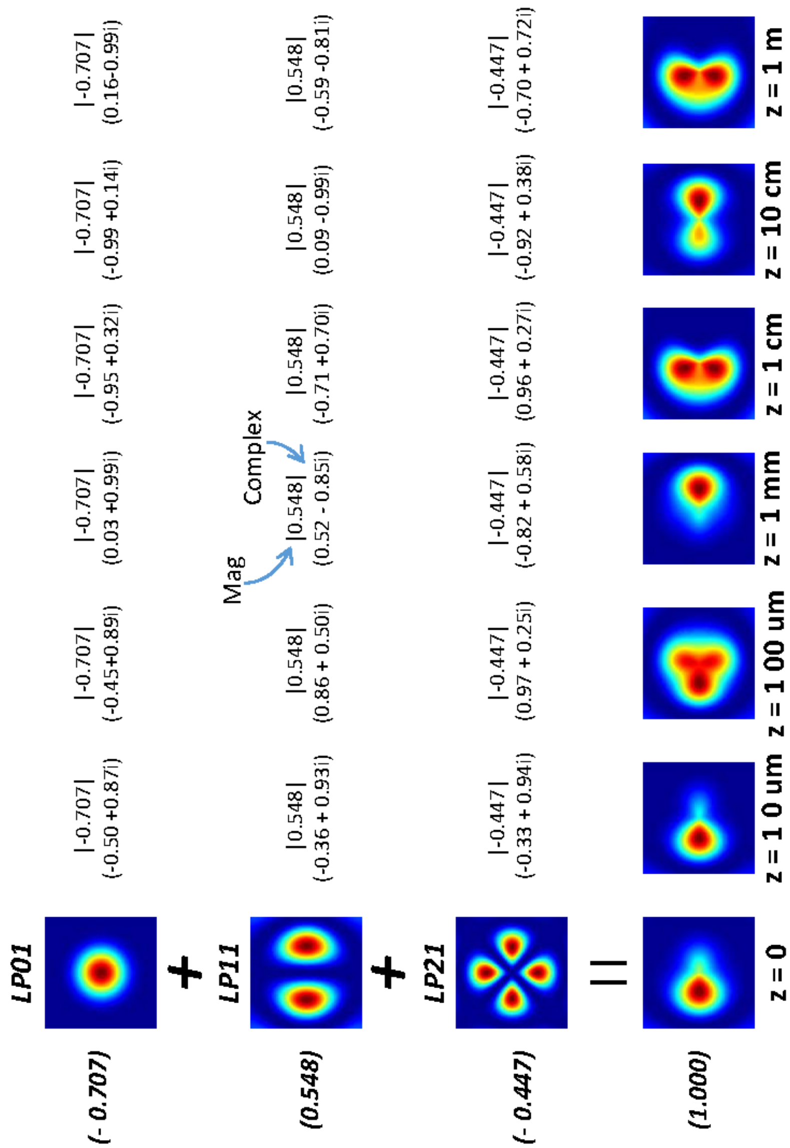

Figure 14: Evolution of the optical field and the optical power distribution in the transverse plane for the example incident field in the text for various z values in the range 0 to 1m. The array of values are the magnitude and phase (expressed as a complex number) of each mode field at a particular z.

the experimentalist, such a splice has loss.

Loss is typically measured in one of two ways: 1) in the forward direction using an optical power meter, and 2) in the backward direction using an optical time-domain reflectometer (OTDR). The power meter measurement is relatively easy to set up but subject to errors due to position and orientation inaccuracies of the optics used to inject light into the fiber. The OTDR measurement is very easy to set up, is not subject to optical alignment errors, and is definitely the preferred approach for splices between identical, singlemode fibers. For nonidentical fibers, an OTDR measurement can exhibit some weird subtleties that must be understood (see Jablon [8], for example, for a discussion of "gainers" in OTDR measurements.)

We can model the splice as a "device" that scatters light from the modes of the incoming fiber (Fiber A) into the modes of the outgoing fiber (Fiber B) as shown in Fig. 15. To simplify the discussion assume the light in fiber A is contained in just one LP mode, say, $A_{l_0 m_0}(x, y)$. When light from fiber A passes through the splice it will scatter into a linear combination of the modes of fiber B,

$$A_{l_0 m_0}(x, y) \longrightarrow \sum_{l,m} c_{lm} B_{lm}(x, y). \tag{26}$$

This is just the mode expansion from Eq.(5) but where we have simplified the notation by lumping all the modes — guided and radiation — into the sum with the understanding that the radiation modes really should be integrated, not summed. We also note that, provided *all* the modes in fiber B are taken into account, then *all* the power from fiber A is accounted for in fiber B and the splice is lossless in the mathematical sense that

$$\sum_{l,m} |c_{lm}|^2 = 1. \tag{27}$$

The weighting coefficients can thus be regarded as optical **scattering coefficients** and we really should write the coefficient as $c_{lm,\, l_0 m_0}$ to keep track of the fact that this coefficient connects mode $(l_0 m_0)$ to mode (lm). Hence **the splice can be characterized by the collection of scattering coefficients** $\{\mathbf{c_{lm,\, l_0 m_0}}\}$ which tells us how much of the light from mode $(l_0 m_0)$ in fiber A ended up in mode (lm) in fiber B. These coefficients are proportional to the overlap integral of Eqs.(6) and (7),

$$|c_{lm,\, l_0 m_0}| \propto \left| \int \int A_{l_0 m_0}(x, y) B_{lm}(x, y) dx dy \right|. \tag{28}$$

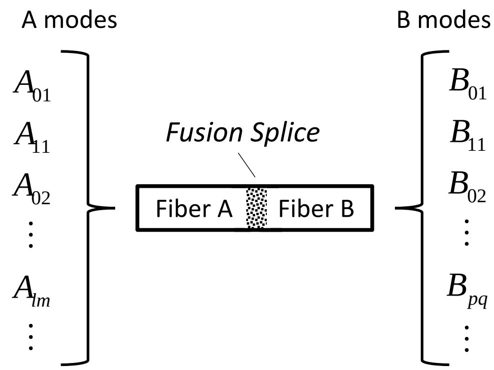

Figure 15: A mode model for a fusion splice between two fibers A and B as a "device" that scatters light from modes in fiber A to modes in fiber B.

Each coefficient is symmetric in the two mode fields $|c_{lm,\,l_0m_0}| = |c_{l_0m_0,\,lm}|$ and is thus independent of the direction of light through the splice. Hence, the **splice loss between any particular mode in fiber A and any particular mode in fiber B is independent of direction**.

Importantly, especially for the discussion in the next section, the functional form of the $(x, y)-$dependence of the expressions for the modes $A_{lm}(x, y)$ depends on the choice of coordinate system. For example, if the origin is shifted to (x_0, y_0) then $A_{lm}(x, y) \to A_{lm}(x - x_0, y - y_0)$.

We next consider two situations, splices between identical singlemode fibers and splices between non-identical or dissimilar fibers.

Identical singlemode fibers Suppose the two fibers A and B are singlemode and identical so they have exactly the same mode solutions $A_{lm}(x, y) = B_{lm}(x, y)$. Assume the fundamental mode $(l, m = 0, 1)$ is the only core-guided mode but recall that a large number of cladding and radiation modes may exist. In the ideal case where the two fibers are perfectly aligned there is no loss and, trivially, no dependence on direction. If the two fibers are not aligned, as shown in Fig. 16(a), they still have identical modes and the functional form of the modes is exactly the same in the coordinate system of each fiber. But from Fig. 16(a) we see that the two coordinate systems are not aligned and hence $A_{lm}(x, y) \neq B_{lm}(x, y)$. From the point of view of fiber B, the incoming fundamental mode from fiber A is not the nice, circularly symmetric, perfectly centered distribution shape of Fig. 16(b) but rather has the oblong, offset shape of Fig. 16(c). For an arbitrary misalignment of fibers we are then effectively back to the situation of Eq.(26) where we must expand an input field from fiber A as a linear combination of all the modes in fiber B. If any of the scattering coefficients other than the one linking the two fundamental modes is nonzero, then the splice has loss. But the scattering coefficient still doesn't depend on direction and so **the splice loss between truly identical, singlemode fibers is independent of direction**.

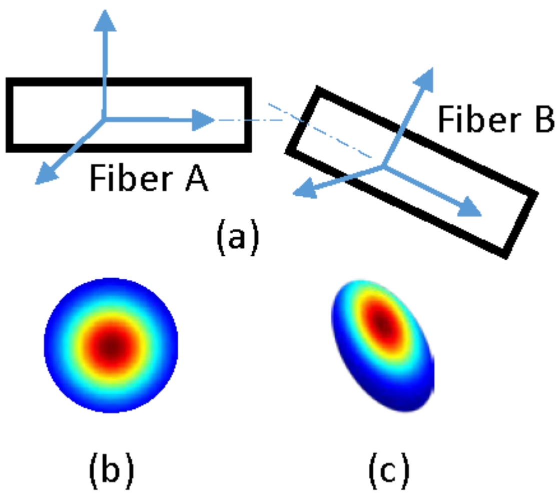

Figure 16: Effect of misalignment in a splice between identical, singlemode fiber. (a) The coordinate systems of the two fibers are tilted and offset with respect to each other. (b) Fundamental mode output of fiber A as viewed in the fiber A coordinate system. (c) Fundamental mode output of fiber A as viewed in the fiber B coordinate system.

Nonidentical fibers For nonidentical fibers we need to be careful about how we define loss. For the purposes of this discussion we will define splice loss in terms of the ratio of power in the core-guided modes of the two fibers. (The measurement of this loss carries a practical danger — some light from fiber A may scatter into cladding-guided modes of fiber B and inadvertently reach the photodetector if precautions are not taken to "strip off the cladding modes.") Again let $A_{lm}(x, y)$ denote the modes of fiber A and now let $B_{pq}(x', y')$ denote the modes of fiber B where we use (x', y') for fiber B since the two coordinate systems may not be identical. To simplify the analysis we'll again assume all the light in fiber A is contained in the fundamental mode A_{01}. Then after the splice the light from fiber A is now contained in a linear combination of all the modes in fiber B

$$\begin{aligned} A_{01}(x,y) &= \sum_{p,q} c_{pq,\,01} B_{pq}(x',y') \\ &= \sum_{\substack{core\\modes}} c_{pq,\,01} B_{pq}(x',y') + \sum_{\substack{cladding+\\radiation\\modes}} c_{pq,\,01} B_{pq}(x',y'). \end{aligned} \tag{29}$$

The ratio of core-guided power into the splice to core-guided power out of the splice is then

$$\left.\frac{p_{in}}{p_{out}}\right|_{A\to B} = \int_{-\infty}^{\infty}\int_{-\infty}^{\infty} \left| \sum_{\substack{core\\modes}} c_{pq01} B_{pq}(x',y') \right|^2 dx'dy'. \tag{30}$$

If now the light were initially contained in the fundamental mode B_{01} of fiber B, propagating in the opposite direction through the splice, then

$$\left.\frac{p_{in}}{p_{out}}\right|_{B\to A} = \int_{-\infty}^{\infty}\int_{-\infty}^{\infty} \left| \sum_{\substack{core\\modes}} c_{lm01} A_{lm}(x,y) \right|^2 dxdy. \tag{31}$$

The right-hand sides of Eqs. (30) and (31) clearly are not equal in general. Hence, **in general, the splice loss between dissimilar fibers depends on direction.**

These results bring up the obvious question "Are any two fibers truly identical?" The practical answer is "No" so some degree of directionality will be observed in the loss of any fiber splice. The directionality may be insignificant for two sections of singlemode fiber taken from the same reel or it may be quite strong such as in the case of a singlemode fiber spliced onto the distal end of a multimode fiber for the purpose of spatial mode filtering.

5.3.3 Mode-Field Diameter

In this section and the next we discuss two useful parameters for singlemode fibers. (A closely-related topic, effective mode area, is discussed in the Appendix.) These are the mode-field diameter (MFD) and the Gaussian approximation to the MFD. As the name implies, mode-field diameter is a measure of the spatial width of the mode and most fiber manufacturers list the MFD at two wavelengths on their data sheet. The MFD is important for two reasons. First, when fusion splicing two non-identical singlemode fibers, knowledge of the MFD of each fiber allows the minimum theoretical splice loss to be estimated. Secondly, today's telecommunications systems increase capacity by pushing to higher optical power levels but with increased power comes the threat of fiber nonlinearities. Signal-to-noise ratio depends on optical power but nonlinearities depend on optical intensity, that is, the power per unit cross-sectional area of the mode. By designing fibers with large MFDs, optical power can be increased while minimizing nonlinear effects.

Two conventions have arisen over the years to define MFD depending on whether we consider the mode pattern in the near field at the fiber endface, or in the far field where measurements are more-easily performed. Artiglia [9] provides a good summary. As shown in Fig. 17 let $E(r)$ denote the near-field radial distribution of the mode field and let $F(p)$ denote the far-field diffracted pattern resulting from $E(r)$ where $p = k \sin\theta$. For splice loss and nonlinearities $E(r)$ is the field that matters but $F(p)$ is more easily determined experimentally. Fortunately, under relatively mild restrictions, the two fields are related by a transform $F(p) = (1/\sqrt{2\pi})\mathcal{H}(E(r))$, where $\mathcal{H}$ denotes Hankel transform. The MFD can thus be defined in either the near- or far-field and in terms of either $E(r)$ or $F(p)$. The near-field MFD, denoted MFD_n, is given by

$$MFD_n = 2\sqrt{2}\left(\frac{\int_0^\infty E^2(r)r^3dr}{\int_0^\infty E^2(r)rdr}\right)^{1/2} = 2\sqrt{2}\left(\frac{\int_0^\infty \left[F'(p)\right]^2 p^3dp}{\int_0^\infty F^2(p)pdp}\right)^{1/2} \tag{32}$$

where $F'(p)$ denotes the derivative of F with respect to p. The first expression on the RHS is called the **"Petermann I"** definition. In the far field,

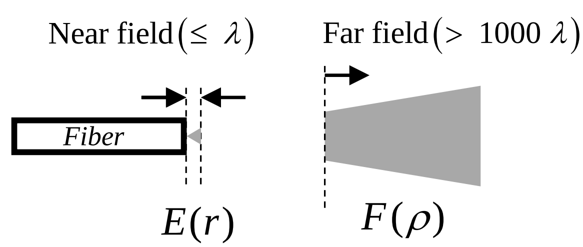

Figure 17: Calculation of the mode-field diameter (MFD) is performed using either the theoretical near-field $E(r)$ or the measured far-field $F(\rho)$.

$$MFD_f = 2\sqrt{2}\left(\frac{\int_0^\infty F^2(p)pdp}{\int_0^\infty F^2(r)p^3dp}\right)^{1/2} = 2\sqrt{2}\left(\frac{\int_0^\infty E^2(r)rdr}{\int_0^\infty \left[E'(r)\right]^2 rdr}\right)^{1/2} \tag{33}$$

Here the first expression on the RHS is called the **"Peterman II"** definition.

For step-index fiber the two definitions yield answers that are quite close but with

$$MFD_f \leq MFD_n \tag{34}$$

However, if we assume the near field can be written as a Gaussian,

$$E_g(r) = A \exp\left(-qr^2\right) \tag{35}$$

then all four expressions give the same result $MFD = MFD_n = MFD_f = 2/\sqrt{a}$. Here, $r = 1/\sqrt{q}$ is the radius at which the *intensity* has dropped to $1/e^2$ of its value at $r = 0$.[1]

The maximum possible linear power transmission coefficient T resulting from a splice between two singlemode fibers having mode-field diameters MFD_1 and MFD_2 is given by Marcuse [10]

$$T = \left(\frac{2 \cdot MFD_1 \cdot MFD_2}{MFD_1^2 + MFD_2^2}\right)^2. \tag{36}$$

5.3.4 Gaussian Approximation to the Fundamental Mode

We found the V-number to be of great utility for determining both electromagnetic modal solutions and the geometric acceptance angle . The V-number appears again in this section for the purpose of approximating the field distribution of the fundamental mode for a singlemode fiber by a Gaussian function. Marcuse [10] has shown that, with quite-good accuracy for step-index fiber, the Bessel-shaped near-field $E(r)$ can be approximated by the Gaussian of Eq. (35) where q is given empirically by

$$\frac{1}{a\sqrt{q}} = 0.65 + \frac{1.619}{V^{3/2}} + \frac{2.879}{V^6}. \tag{37}$$

For a Gaussian of the form $\exp\left(-r^2/w^2\right)$, then the left side of Eq.(37) is simply w/a. Fig. 18 shows the ratio of MFD to core diameter, $2w/2a$, as a function of V. It is seen that, as V decreases, the MFD increases. This is

[1]Note: The integrals in (32) and (33) are evaluated easily using $\int_0^\infty r^n \exp(-ar^2)dr = ((n-1)/2)!/2a^{(n+1)/2}$ for n odd.

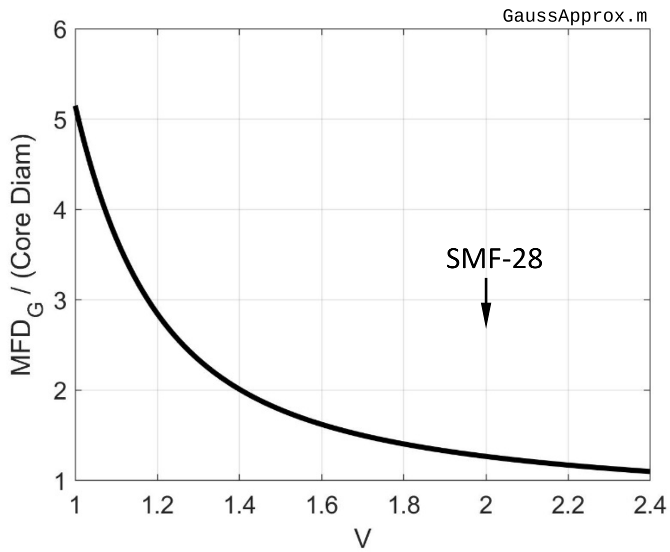

Figure 18: Ratio of MFD in the Gaussian approximation to core diameter as a function of V.

true qualitatively for higher-order modes as well — as the mode approaches cut-off its MFD increases.

Finally, the reader is cautioned that a slightly different form of the Gaussian approximation appears in Marcuse [11]. In that paper, Marcuse sought an approximation that was valid in the more general case of graded-index fibers (of which step-index is a special case). Specifically for step-index fibers, (37) is more accurate.

6 Summary

We have provided a brief introduction to the concept of modes in optical fiber with an emphasis on core-guided modes and, especially, the lowest-order mode or fundamental mode. Some important summary points are:

1. Modes comprises the solutions to Maxwell's equations subject to boundary conditions given by the refractive index profile of the fiber.

2. Mathematically, the complete set of mode solutions comprise a basis, hence, any input field can be written as a complex linear combination of modes.

3. Modes in fiber can be classified as either core-guided modes, cladding-guided modes, or radiation modes.

4. As light in a mode propagates in the fiber, the E-field amplitude distribution in the transverse plane of core-guided modes remains unchanged while the phase accumulates at a rate per meter given by the propagation constant. These two properties make it simple to calculate the mode at any point along the fiber and, together with Summary point 2), allow the total core-guided field to be easily calculated as it propagates in the fiber.

5. The normalized frequency or V-number is probably the most important parameter governing the modal behavior of a fiber. Another important parameter is the so-called normalized propagation constant b. A plot of b vs V provides a set of universal curves that pretty much tell the complete story of the behavior of core-guided modes in fiber, all in a single graph.

6. The mode approach can be used to analyze splice loss. In principle, the splice loss between identical, singlemode fibers is independent of direction of the light but, in practice, some directionality is likely to be present.

7. Using the mode approach a number of important parameters associated with the fundamental mode can be calculated including mode-field diameter, effective mode area, the Gaussian approximation to the fundamental mode, and the relationship between mode amplitude and optical power carried by the mode.

7 Acknowledgments

The authors wish to thank Matthew Mondich and Daniel Nickel for helpful comments and discussions.

A Appendix: Some Details of the Fundamental Mode

In this Appendix we provide details for the calculation of certain parameters associated with the core-guided modes. As overall references we used the original article by Gloge [1], Chap. 3 by Marcuse, Gloge, and Marcatili, "Guiding properties of fibers," in Optical Fiber Communications, S.E. Miller and A.G. Chenowyth (eds.), Academic Press, Orlando, 1979, and the book by Jeunhomme [2]. Compared to that reference material, this Appendix adds value by a) summarizing only the relevant information; b) adding detail and explanation where needed; and c) making direct connections to equations and plots found in the body of this report.

A.1 Form of the Core-Guided Eigenmodes

Core modes in the weakly-guiding approximation are designated LP_{lm} where l is the azimuthal mode number and m is the radial mode number. These modes are nearly linearly polarized in the $x-$ or $y-$directions. From Gloge [1] and Marcuse [5] the dominant transverse E-field components of the LP modes can be written

$$(E_x)_{lm} = \begin{cases} E_l J_l\left(U\frac{r}{a}\right)\begin{pmatrix}\cos l\phi \\ \sin l\phi\end{pmatrix}\exp\left(j\beta_{lm}z\right) & \text{for } r \le a \\ E_l \dfrac{J_l(U)}{K_l(W)} K_l\left(W\frac{r}{a}\right)\begin{pmatrix}\cos l\phi \\ \sin l\phi\end{pmatrix}\exp\left(j\beta_{lm}z\right) & \text{for } r \ge a \end{cases} \tag{38}$$

where

$$U = a\sqrt{k^2 n_{co}^2 - \beta_{lm}^2}, \tag{39a}$$

$$W = a\sqrt{\beta_{lm}^2 - k^2 n_{cl}^2}, \tag{39b}$$

and where E_l is an amplitude parameter (Volts/m), $\beta_{lm} = kn_{eff,lm}$ is the mode propagation constant and $k = 2\pi/\lambda$. For the fundamental mode, $E_{l=0}$ is the field strength at the origin. U and W are sometimes referred to as the **scalar mode parameters**.

In the above equation subscript x indicates the Cartesian component of the E-field and the field is expressed in terms of cylindrical coordinates (r, ϕ, z) and A is the mode amplitude. Here J and K are Bessel functions of integer order. (In Matlab, they are besselj(l, x) and besselk(l, xr) and in

Mathematica they are BesselJ[l,x] and BesselK[l,x].) Choosing either $\cos l\phi$ or $\sin l\phi$ yields a valid solution so both must be stated explicitly in order for the solution set to be complete. And there is another set of solutions just like (38) for the orthogonal polarization component E_y. Either in plotting the field distribution of the mode or in performing calculations, typically only one version of one polarization state is used. For example, the mode pictures in Fig. 6 represent a choice of one state of polarization E_x or E_y and one choice of either $\cos l\phi$ or $\sin l\phi$. But bear in mind that in doing the mode expansion for, say, an incident field, ALL the solutions must be included.

Inside the core radius the field is proportional to $J_l(Ur/a)$ which remains finite at the origin while, outside the core, the mode field is proportional to $K_l(Wr/a)$ which decays exponentially to zero as r goes to infinity. Solving for the modes then requires that the scalar mode parameters satisfy two constraints

$$U^2 + W^2 = V^2, \tag{40a}$$

$$U\frac{J_{l+1}(U)}{J_l(U)} = W\frac{K_{l+1}(W)}{K_l(W)} \tag{40b}$$

where V is the V-number. The second equation is the characteristic equation or eigenvalue equation and it must be solved to obtain values for U and W. Unfortunately, the eigenvalue equation cannot be solved analytically and even after the great simplification arising from introduction of the LP mode concept by Gloge. But it turns out that either U or W can be approximated as a function of V and then the other parameter (W or U) can be determined from (40a). We now compare two approximation approaches that have appeared in the literature. We will limit the analysis to the fundamental mode ($l = 0$) for which the eigenvalue equation becomes

$$U\frac{J_1(U)}{J_0(U)} = W\frac{K_1(W)}{K_0(W)}. \tag{41}$$

A.2 Approximations for the Scalar Mode Parameters

Tables providing numerically accurate values for U and W for various values of V are given in Jeunhomme [2] (Table 1.1, where his u is our U and his v is our W), and in Snyder and Love [7] (Table 14-4, where their $\tilde{U}$ and $\tilde{W}$ correspond to our U and W, respectively). Both Tables are presumed accurate. Figure 19 show U and W as a function of V. At low V-numbers, W is small compared to U. Since $W = a\sqrt{\beta^2 - k^2 n_{cl}^2}$ this indicates that the mode effective index is close to the cladding index in the low-V regime, while at larger V values, the mode index gets closer to the core index.

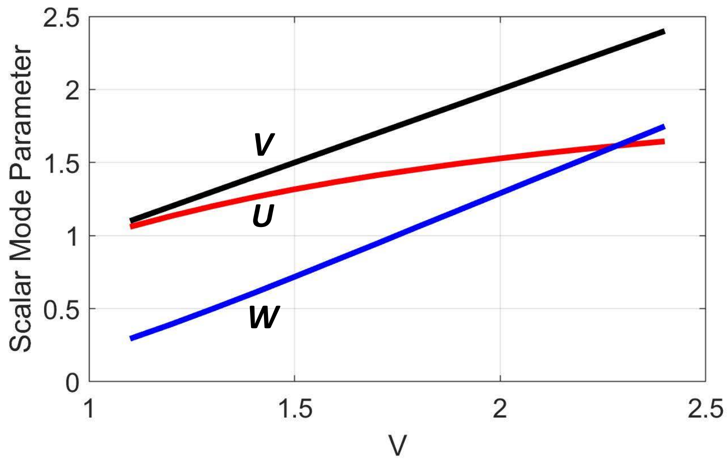

Figure 19: The scalar mode parameters U and W as a function of the normalized frequency V where $U^2 + W^2 = V^2$. V itself is also plotted for comparison. For SMF-28 fibers $V \simeq 2.0$.

If you're stuck on a deserted island and don't have access to a table of scalar mode parameters two approximations exist that can be used in a pinch. One was given by Marcuse, Gloge, and Marcatilli, Chapter 3 in Miller and Chenowyth [3], and provides an approximation for $U(V)$ and from which $W(V)$ is then obtained using (40a)

$$U_{MGM}(V) = \frac{\left(1+\sqrt{2}\right)V}{\left[1+(4+V^4)^{1/4}\right]}, \tag{42a}$$

$$W_{MGM}(V) = \sqrt{V^2 - U_{MGM}(V)^2}, \tag{42b}$$

where the subscript indicates Marcuse, Gloge, and Marcatilli. The other is an approximation for $W(V)$ given by Jeunhomme [2] and from which $U(V)$ is obtained, again, using (40a),

$$W_J(V) = 1.1428V - 0.9960, \tag{43a}$$

$$U_J(V) = \sqrt{V^2 - W_J(V)^2}, \tag{43b}$$

where subscript "J" indicates Jeunhomme. To check the accuracy of the approximations we first chose a value for V, then found the correct corresponding U and W from the Table, and then calculated the approximation error $Error = X - X_{MGM,J}$ where $X = U, W$.

Alternatively, the two parameters can also be obtained numerically by finding the U value $U = U_{Num}$ that minimizes the difference

$$diff = \left| U \frac{J_1(U)}{J_0(U)} - \left(\sqrt{V^2 - U^2}\right) \frac{K_1\left(\sqrt{V^2 - U^2}\right)}{K_0\left(\sqrt{V^2 - U^2}\right)} \right|, \tag{44}$$

and then calculating $W = \sqrt{V^2 - U^2}$. In this way we find the (U, W) values that come close to satisfying the characteristic equation (40b) as shown in Fig. 20.

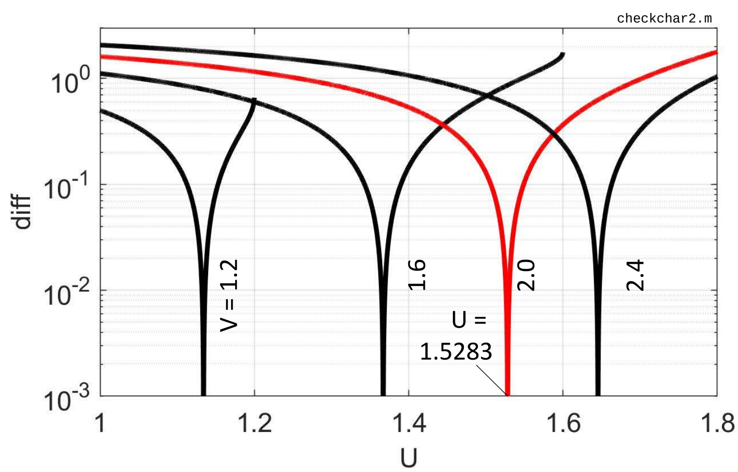

Figure 20: Some examples of graphical solutions to the eigenvalue equation. The red curve corresponding to $V = 2.0$, typical of SMF-28 fibers, has solutions $U = 1.5282$, $W = \sqrt{V^2 - U^2} = 1.2902$.

These results are summarized in Fig. 21. We see that the Jeunhomme approximation is quite good over most of the range shown while the MGM approximation is not quite as good. The numerical approach provides excellent results.

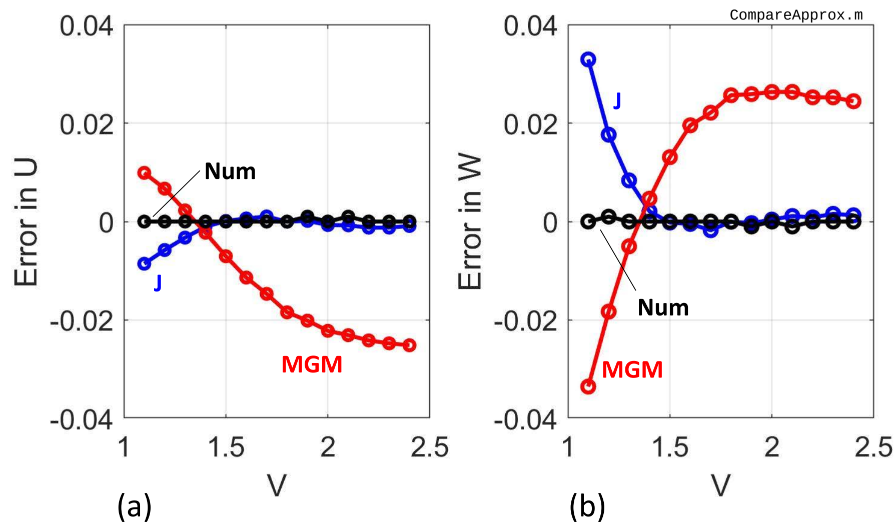

Figure 21: Approximation errors using each approach for (a) U and (b) W. For SMF-28 fibers, $V \simeq 2.0$.

A.3 Amplitude and Power of the Fundamental Mode

The mode amplitude E_l and the optical power P_l in the $l-th$ mode are related by [1]

$$E_l = \left[\frac{4Z_0W^2}{e_l \pi n_{co} a^2 V^2 \left|J_{l-1}(U) J_{l+1}(U)\right|}\right]^{1/2} \sqrt{P_l} \tag{45}$$

where the amplitude E_l is in units Volts/m, $Z_0 = \sqrt{\mu_0/\epsilon_0} = 377\,\Omega$ is the characteristic impedance of free space, and

$$e_l = \begin{cases} 2 & \text{for} \quad l = 0, \\ 1 & \text{for} \quad l \neq 1. \end{cases} \tag{46}$$

For the fundamental mode ($l = 0$),

$$E_0 = \left[\frac{2Z_0W^2(V)}{\pi n_{co} a^2 V^2 J_1^2(U(V))}\right]^{1/2} \sqrt{P_0} \tag{47}$$

where $U(V) = \sqrt{V^2 - W^2(V)}$ and we have used $J_{-n}(x) = (-1)^n J_n(x)$. As an example, suppose we use the Jeunhomme approximation $W(V) =$

$1.1428V - 0.9960$ and choose fiber parameters typical of an SMF-28-type fiber, $n_{co} = 1.448$ and $a = 4.1\,\mu m$ then, for $P_{01} = +10$ dBm, the dependence of E_0 on V is plotted in Fig. 22. We see that, for fixed power, as V decreases, the mode is less tightly bound (recall from Fig. 18 that the MFD increases as V decreases) and, hence, the same power is spread over a larger mode cross-sectional area. Also note that, even for the relatively modest power level of 10 mW, the field in the fiber center is approaching 1 MVolt/m!

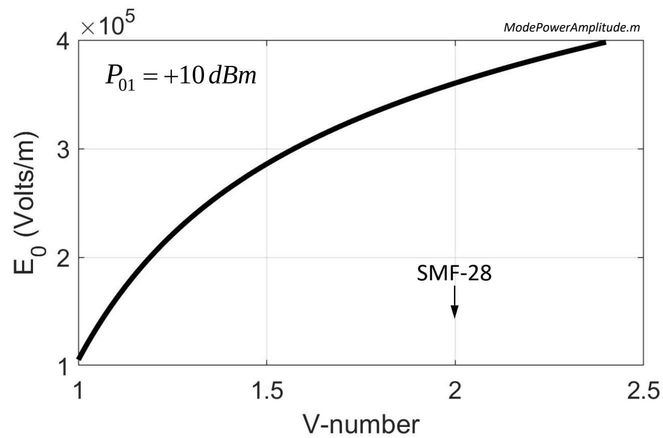

Figure 22: For the fundamental mode, the dependence of the mode field amplitude E_0(Volts/m) as a function of V-number for mode power $P_{01} = 10\,mW$, $a = 4.1\,\mu m$, and $\lambda = 1550\,nm$

.

A.4 Effective Area of the Fundamental Mode

An important fiber parameter for understanding nonlinear effects in fiber is the effective mode area A_{eff} defined by

$$A_{\text{eff},\,lm} = \frac{\left(\int_{-\infty}^{\infty}\int_{-\infty}^{\infty} |LP_{lm}(x,y)|^2\,dxdy\right)^2}{\int_{-\infty}^{\infty}\int_{-\infty}^{\infty} |LP_{lm}(x,y)|^4\,dxdy}. \tag{48}$$

If we approximate the fundamental mode shape by a Gaussian

$$LP_{01}(x,y) = \exp\left(\frac{-x^2 - y^2}{w^2}\right) \tag{49}$$

then, very nicely, $A_{\text{eff},01} = \pi w^2$. And we can then use the approximation (37) to express $A_{\text{eff},01}$ as a function of V for the fundamental mode as

$$A_{\text{eff},01}(V) = \pi a^2 \left(0.65 + \frac{1.619}{V^{3/2}} + \frac{2.879}{V^6}\right)^2 . \tag{50}$$

Figure 23 is a plot of $A_{\text{eff},01}$ vs V for core radius $a = 4.1\,\mu m$.

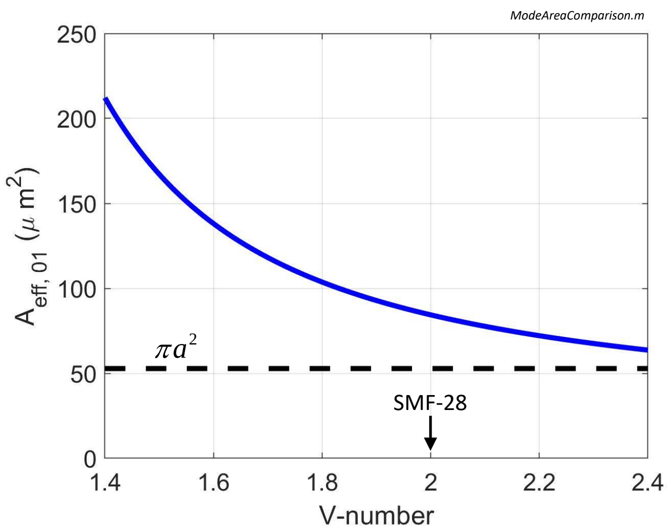

Figure 23: For the fundamental mode, the dependence of the mode effective area $A_{\text{eff},01}$ as a function of V-number. Also shown is the core area πa^2. Both curves are for core radius $a = 4.1\,\mu m$.

References

[1] D. Gloge. "Weakly Guiding Fibers". *Appl. Opt.* **10**(10) (1971), pp. 2252–2258.

[2] L.B. Jeunhomme. Single-Mode Fiber Optics. Marcel Dekker, 1983.

[3] S.E. Miller and A.G. Chynoweth. Optical Fiber Telecommunications. Academic Press, 1979.

[4] H.-G. Unger. Planar Optical Waveguides and Fibres. Clarendon Press, Oxford, 1977.

[5] D. Marcuse. Theory of Dielectric Optical Waveguides, 2nd Ed.. Academic Press, 1991.

[6] D. Marcuse. Fiber-Optic Communication Systems. Wiley, 1992.

[7] A.W. Snyder and J.D. Love. Optical Waveguide Theory. Chapman and Hall, 1991.

[8] A.D. Yablon. Optical Fiber Fusion Splicing. Springer, 2005.

[9] M. Artiglia, G. Coppa, P. Di Vita, M. Potenza, and A. Sharma. "Mode field diameter measurements in single-mode optical fibers". *J. Lightwave Technol.* **7**(8) (1989), pp. 1139–1152.

[10] D. Marcuse. "Loss Analysis of Single-Mode Fiber Splices". *Bell Systems Technical Journal* **56**(5) (1977), pp. 703–718.

[11] D. Marcuse. "Gaussian approximation of the fundamental modes of graded-index fibers". *J. Opt. Soc. Am.* **68**(1) (1978), pp. 103–109.